Pulse compression and beam focusing with segmented diffraction gratings in a high-power chirped-pulse amplification glass laser system

Hideaki Habara,[1,2,*] Guang Xu,[1,4] Takahisa Jitsuno,[1] Ryosuke Kodama,[1,2] Kenji Suzuki,[1] Kiyonobu Sawai,[1] Kiminori Kondo,[1,5] Noriaki Miyanaga,[1] Kazuo A. Tanaka,[1,2] Kunioki Mima,[1] Michael C. Rushford,[3] Jerald A. Britten,[3] and Christopher P. J. Barty[3]

[1]*Institute of Laser Engineering, Osaka University, 2-6, Yamada-oka, Suita, Osaka 565-0871, Japan*

[2]*Graduate School of Engineering, Osaka University, 2-1, Yamada-oka, Suita, Osaka 565-0871, Japan*

[3]*Lawrence Livermore National Laboratory, L-470, 7000 East Avenue, Livermore, California 94550, USA*

[4]*Current address: National Laboratory on High Power Laser and Physics, Shanghai Institute of Optics and Fine Mechanics, Chinese Academy of Science, 390 Qinghe Road, Jiading, Shanghai 201800, China*

[5]*Current address: Advanced Photon Research Center, Japan Atomic Energy Agency, 8-1-7, Umemidai, Kizu, Kyoto 619-0215, Japan*

**Corresponding author: habara@ile.osaka-u.ac.jp*

Received January 20, 2010; revised March 30, 2010; accepted March 31, 2010; posted May 5, 2010 (Doc. ID 121180); published May 19, 2010

Segmented (tiled) grating arrays are being intensively investigated for petawatt-scale pulse compression due to the expense and technical challenges of fabricating monolithic diffraction gratings with apertures of over 1 m. However, the considerable freedom of motion among grating segments complicates compression and laser focusing. We constructed a real compressor system using a segmented grating for an 18 cm aperture laser beam of the Gekko MII 100 TW laser system at Osaka University. To produce clean pulse shapes and single focal spots tolerant of misalignment and groove density difference of grating tiles, we applied a new compressor scheme with image rotation in which each beam segment samples each grating segment but from opposite sides. In high-energy shots of up to 50 J, we demonstrated nearly Fourier-transform-limited pulse compression (0.5 ps) with an almost diffraction-limited spot size (20 μm).

OCIS codes: 050.0050, 140.0140.

For new-generation petawatt laser systems based on the chirped-pulse amplification technique with kilojoule glass laser amplifiers, for example, LFEX [1] or Omega-EP [2], the required diffraction-grating-size pulse compression exceeds 1 m owing to the extreme fluence. There are several difficulties involved in the manufacture of large-scale gratings in terms of maintaining substrate flatness, coating and linewidth uniformity, and holographic phase uniformity. A segmented (tiled) grating array is one of the realistic solutions to such problems [3]. A segmented grating, however, has considerable freedom of motion, which complicates both pulse compression and beam focusing. For example, grating tip and tilt errors give rise to separation of the beam spot in the far-field pattern, and slight piston and lateral motion errors among gratings cause interference on the pulse shape and beam pattern [4–6]. In addition, a small mismatch of groove density among element gratings leads to considerable separation of focal pattern in many spots owing to changes of diffraction angles. Several techniques have been proposed to adjust segmentation based on measurements of interference of the beam pattern and on interferometric techniques [7–9].

Recently, the image rotation technique has been proposed and demonstrated to compensate the groove density mismatch between two gratings [1,10,11]. The diffracted beam from the segment grating is flipped horizontally by mirrors, and then the reversed image beam reenters the same segment grating from the opposite side of the first diffraction. In this scheme, one beam segment experiences both gratings, so that the groove density mismatch is naturally canceled. Using this technique, we built a pulse compressor with a segmented grating for Gekko MII (GMII) 100 TW laser system at Osaka University. In this Letter, we report that the compressed pulse width is stably achieved close to the Fourier transform limit in high-power shots. Also, we successfully obtain a small single focal spot of nearly 20 μm, corresponding to 10^{19} W/cm^2 of focused intensity.

The GMII system consists of a Ti:sapphire oscillator operating at 1 μm, a pulse stretcher, a preamplifier based on optical parametric chirped-pulse amplification (OPCPA), an Nd:glass amplifier, a pulse compressor, and an off-axis parabolic focusing mirror. An 80 fs pulse from the oscillator is stretched to 1.3 ns with 10 nm spectral width in FWHM. After three-stage OPCPA using beta-barium-borate crystals, the pulse energy is increased to the millijoule level. The pulse contrast is enhanced by a Pockels cell and is injected into a rod and disk glass amplifier chain to be amplified up to 50 J. The high-energy pulse is then compressed at dielectric coated gratings to be a temporal duration of several hundred femtoseconds and is finally focused onto a target with a $F/3.3$ off-axis parabolic mirror.

Figure 1 shows the optical layout inside the compressor chamber. The gratings in this system have a dielectric coating with 1740 lines/mm. The size of one grating is 40 cm × 20 cm. Although the beam path appears somewhat complicated, the compressor layout is basically a double-pass arrangement composed of two grating pairs (G1-G2/G3 and G2/G3-G4) with image rotation provided by mirrors M2 and M3. The incident beam arrives on G1 with 72.5° incident angle and is diffracted to the G2/G3 segments with a travel distance of 1.35 m. This segment covers a 40 nm bandwidth by taking into account the

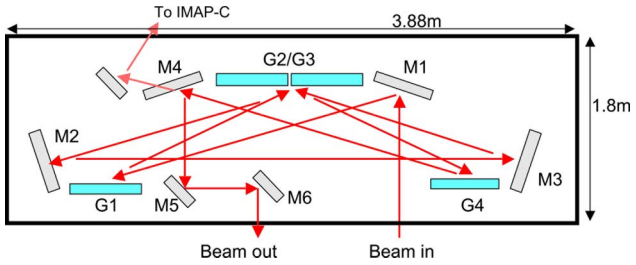

Fig. 1. (Color online) Schematic view of compression chamber. The laser pulse travels, in turn, to mirror 1 (M1), grating 1 (G1), G2/G3 segments, M2, M3, G3/G2, G4, M4, M5, and M6.

horizontal output beam size (10.5 cm), which is wide enough for the amplified laser beam with a 3–4 nm spectral width (FWHM). A diffracted beam from left segment G2 (or right segment G3 in another case) is then horizontally inverted to arrive at right segment G3 (or left segment G2), and goes into a second grating pair with the same incident angle and distance. Therefore, this beam-path arrangement is a modification of that of a diamond-shaped compressor of the LFEX PW laser [1,10]. After compression, the laser pulse is delivered into the interaction chamber via mirrors M4, M5, and M6. Transmitted light through M4 is used to monitor the pulse shape with an autocorrelator, the prepulse level with a p-i-n photodiode, and the far-field pattern with a CCD.

As an initial alignment of a segment, we mainly utilize three sensors [12]: a laser line generator for initialization of the plumbed positions of all optics and surface rotation of gratings, a two-dimensional motion sensor for adjustment of piston error within 1 μm, and a three-axis motion sensor (capacitance detector) for monitoring the motion of the grating in vacuum with 1 nm precision. For precise control of grating segments, the grating holder has five axes motions (three for piston motion, one for surface rotation, and one for translation motion along the surface) with 5 nm resolutions. Using these alignment tools, we obtained a clean pulse shape with a 300 fs duration (10 nm spectral width) and a single small spot size (1.4× diffraction limit) by simply adjusting a horizontal tilt of the segment grating for the OPCPA light coming through the whole amplifier chain. The focusing position and pattern are very stable, except for an infrequent split of the spot that is possibly due to rapid modulation of the spectral shape coming from the OPCPA timing jitter (<2 ns) in our system.

In the image rotation layout, a zero-order surface reflection at the segment grating becomes a significant problem, because the reflected pulse at G2/G3 is diffracted at G4 (single-pass compression with the same distance as double pass) and is delivered to the focal point in the same path as the desired compressed pulse. This generates compressed prepulse. In a similar manner, postpulses are created according to a path from G1, G2/G3, M2, M3, and G2/G3 through G4 and a subsequent path with a round-trip time among G2/G3, M2, M3, and G2/G3. We measured −1 order diffraction efficiencies of 92%–95% and zero-order reflection efficiencies of 5%–8% for 72.5° incidence in 1 μm light. The intensities of both the prepulse and the first postpulse were, therefore, estimated to be 10^{18} W/cm^2 as the maximum. To avoid the formation of plasma before the main pulse, we separate the diffracted and the surface reflected beam at the focal point by changing the second incident angle (from M3 to G2/G3) by slightly moving mirrors M2 and M3 (of the order of a few milliradians), keeping with the beam centering on the segment. This breaking of the symmetry of the compressor causes a slight change of dispersion between the left-half and right-half compressors, but it can easily be compensated by adjusting the grating distance in the pulse stretcher (to be $\phi_{\mathrm{com}-R}+\phi_{\mathrm{com}-L}=\phi'_{\mathrm{str}}$). On the other hand, one can expect that the larger tilting angles of mirrors leads to a larger separation distance of the prepulse and the main pulse on the focusing point. However, it also causes beam splitting into two spots due to interference of the right and left sides of the beam. With the restriction of minimum separation derived from the target size in the plasma experiment, we decided to separate by a few millimeters to obtain a single spot and large separation simultaneously. Figure 2 shows a streak image (time axis from top to bottom) of a compressed pulse (a) before and (b) after the 3.2 mm separation of the prepulse and the main pulse on the focus points. As shown in Fig. 2(a), there is clearly a prepulse (top line) and a postpulse (bottom), as well as the main pulse (center), with about a 1/10 contrast ratio at ±21.3 ns from the main pulse, of which timing is exactly the same as the round-trip time of the optical path among G2/G3, M2, and M3. Accordingly, no subpulses are observed after separation.

Under these conditions, we successfully obtained a short pulse width and a small single focal spot at a high-energy shot of up to 50 J. Figure 3(a) shows a compressed pulse shape with 24 J output energy detected with a single-shot second-order autocorrelator. The pulse width is about 470 fs (FHWM), which is nearly the Fourier transform limit, corresponding to a spectral width of 3.5 nm. The shot-to-shot fluctuation on the pulse width is about 460–600 fs. Nevertheless, the spectral width after amplification is almost constant owing to gain narrowing. On the other hand, the focusing pattern is sensitive to the horizontal tilting and surface rotation error of the segment grating. The focal beam pattern completely separates into two spots for 2.5 and 0.5 μrad horizontal tilting and rotation error, respectively. However, the piston and lateral motion and vertical tilting do not affect the pulse shape and focusing pattern owing to image rotation. Adjusting these errors by checking the far-field pattern using a low-energy full-aperture pulse before the main shot, we obtained a single spot in a typically 20 μm spot diameter. Figure 3(b) indicates an example of the

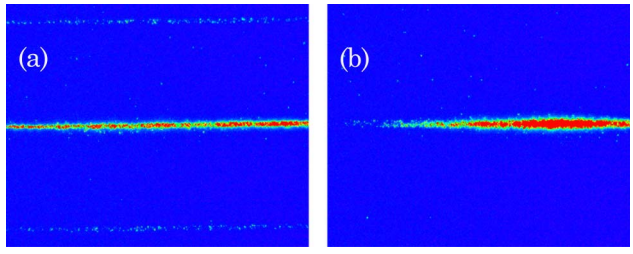

Fig. 2. (Color online) Streak image (a) before and (b) after the beam separation of prepulse and postpulse. The vertical axis represents time from 0 (top) to 50 ns (bottom), and the horizontal axis is the space with the full span of detector.

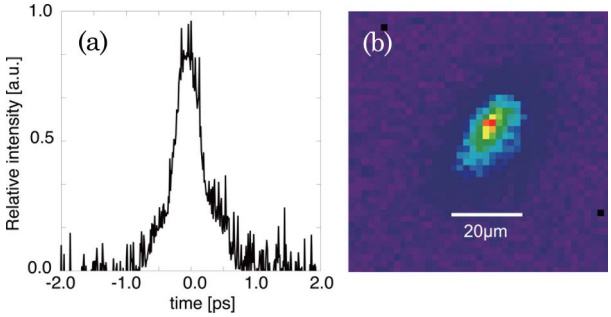

Fig. 3. (Color online) (a) Typical compressed pulse shape taken with a second-order autocorrelator. The pulse width is 470 fs on 24 J laser output energy. (b) Typical x-ray image taken with a pinhole camera for an Al plane target irradiated with 5 J of laser energy.

focusing pattern taken with an x-ray pinhole camera at about 40° of view angle from the target normal direction when a 5 J laser pulse is irradiated on a flat Al target. The spot size is about 20 μm × 25 μm (FWHM), which is about 2–2.5 times the diffraction limit. Even when the laser energy increases to 50 J, we obtain a similar focal pattern with fluctuations of about 20–30 μm in diameter.

From the viewpoint of a laser-plasma experiment, the existence of preformed plasma created by a high-level prepulse is a significant problem. To estimate the size of the plasma, we use an optical interferometric technique that uses a probe beam with 5 ps temporal windows. In the result, no fringe shift on the target surface is observed up to 150 ps before the main pulse. Thus, we conclude that the target ions are almost immobile until the time of interaction with the main pulse, considering ion sound speed. From the observations with an optical streak camera (temporal windows of up to ±25 ns) and an autocorrelator (±5 ps), we obtained no intense prepulse or pedestal (detection limit of contrast = 1/100), so that one can expect no preformed plasma before interaction.

In summary, we constructed a high-energy and intense laser system using a segmented grating array in the pulse compressor. A 50 J/100 TW pulse is stably available in the system. The compressed pulse and the focusing size are typically 500 fs and 20 μm in diameter at higher-energy shots, corresponding to 10^{19} W cm^2 of laser intensity.

We gratefully acknowledge the Japan Society for the Promotion of Science (JSPS) for their financial support of this system through the Creative Scientific Research program. We also thank the FIREX project team of the Institute of Laser Engineering (ILE) for their financial and technical support for the segment grating.

References

1. N. Miyanaga, H. Azechi, K. A. Tanaka, T. Kanabe, T. Jitsuno, J. Kawanaka, Y. Fujimoto, R. Kodama, H. Shiraga, K. Knodo, K. Tsubakimoto, H. Habara, J. Lu, G. Xu, N. Morio, S. Matsuo, E. Miyaji, Y. Kawakami, Y. Izawa, and K. Mima, J. Phys. IV **133**, 81 (2006).
2. J. H. Kelly, L. J. Waxer, V. Bagnoud, I. A. Begishev, J. Bromage, B. E. Kruschwitz, T. J. Kessler, S. J. Loucks, D. N. Maywar, R. L. McCrory, D. D. Meyerhofer, S. F. B. Morse, J. B. Oliver, A. L. Rigatti, A. W. Schmid, C. Stoeckl, S. Dalton, L. Folnsbee, M. J. Guardalben, R. Jungquist, J. Puth, M. J. Shoup III, D. Weiner, and J. D. Zuegel, J. Phys. IV **133**, 75 (2006).
3. V. Mazzacurati and G. Ruocco, Opt. Commun. **76**, 185 (1990).
4. T. J. Zhang, M. Yonemura, and Y. Kato, Opt. Commun. **145**, 367 (1998).
5. T. Harimoto, Jpn. J. Appl. Phys. **43**, 1362 (2004).
6. T. J. Kessler, J. Bunkenburg, H. Huang, A. Kozolv, and D. D. Meyerhofer, Opt. Lett. **29**, 635 (2004).
7. J. Bunkenburg, T. J. Kessler, W. Skulski, and H. Huang, Opt. Lett. **31**, 1561 (2006).
8. L. Zeng and L. Li, Opt. Lett. **31**, 152 (2006).
9. Y. Hu, L. Zeng, and L. Li, Opt. Commun. **269**, 285 (2007).
10. M. C. Rushford, J. A. Britten, C. P. J. Barty, T. Jitsuno, K. Kondo, N. Miyanaga, K. A. Tanaka, R. Kodama, and G. Xu, Opt. Lett. **33**, 1902 (2008).
11. G. Xu, H. Habara, K. Suzuki, K. Sawai, T. Jitsuno, R. Kodama, K. A. Tanaka, N. Miyanaga, M. C. Rushford, J. A. Britten, and C. P. J. Barty, "The property of paired tiled gratings in dual-side incident laser pulse compressor," submitted to Opt. Lett.
12. H. Habara, G. Xu, T. Jitsuno, R. Kodama, K. Suzuki, K. Sawai, C. P. J. Barty, T. Kawasaki, H. Kitamura, K. Kondo, K. Mima, N. Miyanaga, Y. Nakata, H. Shiraga, K. A. Tanaka, K. Tsubakimoto, and M. C. Rushford, J. Phys. Conf. Ser. **112**, 032017 (2008).